

Characterization of Bonding and Crystalline Phases in Fluxed Pellets Using Peat Moss and Bentonite as Binders

S.C. PANIGRAHY, B.C. JENA, and M. RIGAUD

Pellets in the basicity range of 0.2 to 1.6 were produced from specular hematite concentrates using bentonite or peat moss as a binder. Specific pellet basicities were achieved through the addition of (1) limestone and (2) a combination of dolomite and limestone. Mineralogical study and microanalysis of the bonding and crystalline phases were done using scanning electron microscopy (SEM) and energy dispersive spectroscopy (EDS). In limestone-fluxed pellets with bentonite as a binder, although formation of calcium ferrite was noted at the basicity of 0.8, its formation in appreciable quantities was delayed until the basicity of 1.6. For the pellets produced with a combination of dolomite and limestone, even at the basicity of 1.6, only minor amounts of this phase were present. In these pellets, some magnesioferrites were formed which did not conform to the stoichiometric composition ($\text{MgO}\cdot\text{Fe}_2\text{O}_3$), but they were quite deficient in MgO. The silicate glass phases, which essentially provided the bonding in the pellets, showed a two-zone structure: (1) magnesian-ferruginous and (2) glass containing high quantities of Si and Ca. However, in pellets with only limestone addition, the zoned structure was less prevalent, probably due to low Mg content. The results indicate that using peat moss in conjunction with limestone, pellet sticking can be minimized at higher basicities. The factors influencing the pellet bonding and the change in the physical and chemical properties of these pellets are discussed.

I. INTRODUCTION

IN recent years, increasing attention has been given to the use of fluxed pellets as blast furnace iron-bearing burden material. The reason is that suitably produced fluxed pellets can meet progressively stringent quality requirements in terms of physical strength, reduction behavior at low and high temperatures, swelling characteristics, softening temperature, and narrow range of temperature within which softening takes place. In general, the quality of pellets is affected by the type and nature of ore or concentrate, gangue and other additives, and their subsequent treatment to produce pellets. These factors result in variation in the physicochemical properties of coexisting phases, structure, distribution, number of pores, *etc.*, in the pellets. The properties of the pellets are, therefore, largely governed by the form and degree of bonding achieved between ore particles and also by the stability of these bonding phases during the reduction of iron oxides. Hence, characterization of the bonding and crystalline phases is of prime importance in understanding the basis for the production of pellets of desired quality.

A limited number of investigations have been done on the bonding in fluxed hematite pellets in the basicity range of 0.5 to 1.0.^[1-7] It is important to note that the conditions and parameters to be controlled are typical of a given concentrate/ore. It is in this context that this research was undertaken for a typical Canadian specular hematite.

In general, the bonding in fluxed pellets is achieved primarily through melt formation during induration. The bonding phase consists mainly of silicates formed from the melt. The various components contributing to melt formation are the gangue of the concentrate, lime and magnesia of the fluxes, bentonite, and iron oxides. Lime and magnesia react with the gangue and/or with the iron oxides. When they react with the gangue, they form part of the intergranular melting phase. The lime also simultaneously reacts with Fe_2O_3 to form different calcium ferrites. These melting phases interact with each other and dissolve a variable amount of iron oxides. While very fine particles of the ore components are easily dissolved, the larger ore particles are attacked at the acute angles and faces, causing a certain amount of surface smoothing. On cooling, the iron oxides and their compounds precipitate from the melt, and calcium ferrites and silicates of various compositions are formed depending on the local chemistry.

In this paper, the effects of basicity, the type of flux (limestone and dolomite), and the type of binder (bentonite and peat moss) on the bonding mechanism of pellets produced from specular hematite concentrates are examined. The changes in both physical and reduction properties of pellets are also discussed.

Special emphasis has been placed on using peat moss as a binder as it is noncontaminating and is abundantly available near the iron ore mines in Quebec.

II. EXPERIMENTAL

A. Raw Materials

The chemical compositions of the raw materials used for this study are given in Table I. In this paper, all compositions and additions of all raw materials are given in

S.C. PANIGRAHY, Research Scientist, and M. RIGAUD, Professor, are with the Department of Metallurgical Engineering, École Polytechnique, Montreal, PQ H3C 3A7, Canada. B.C. JENA, Postdoctoral Fellow, is with the Department of Metallurgical Engineering, McGill University, Montreal, PQ H3A 2A7, Canada.

Manuscript submitted January 27, 1989.

Table I. Chemical Composition of Raw Materials

Raw Material	Size	Fe	SiO ₂	Al ₂ O ₃	CaO	MgO	Na ₂ O	K ₂ O
Iron ore	65 pct, -44 μm	65.35	5.05	0.33	0.033	0.03	—	—
Dolomite	65 pct, -44 μm	0.22	1.0	0.14	30.30	20.75	—	—
Limestone	65 pct, -44 μm	—	2.0	0.6	53.00	0.5	—	—
Bentonite	69 pct, -44 μm	2.41	64.43	18.42	1.5	2.00	2.22	0.60
Coke breeze (14.1 pct ash)	67 pct, -44 μm	2.45	5.45	3.03	0.98	0.03	—	—

weight percent except where indicated. The pellet designations and weight percents of binder/fluxes in the raw mix are given in Table II. The pellet designations are defined as follows: the prefix letter "L" refers only to limestone and "D" refers to a combination of dolomite and limestone addition; the suffix letters "B" and "P" refer to bentonite and peat moss additions, respectively, at specific basicity levels. The pellets were produced at basicities ($B = (\text{CaO} + \text{MgO})/(\text{SiO}_2 + \text{Al}_2\text{O}_3)$) of 0.2, 0.8, 1.3, and 1.6. To assess the effect of binders, pellets were produced with addition of either bentonite (1 pct) or peat moss (3 pct). At a low basicity of 0.2, the pellets were produced with 1.8 pct dolomite addition, following the practice adopted at some Quebec pelletizing plants while producing acid pellets. All other specific basicity levels were obtained with (1) limestone and (2) a combination of dolomite (9 pct), the rest being limestone. In the text, the pellets produced with either dolomite or a combination of dolomite and limestone have been referred to as dolomite-fluxed pellets. Addition of 9 pct dolomite corresponded to a MgO content of approximately 2.0 pct in fired pellets. In the case of pellets produced with peat moss addition, it was found necessary to treat the peat moss with small amounts of NaOH prior to mixing with other raw materials. It is believed that NaOH changes the surface characteristics of peat moss in a certain pH range and enhances its capacity for binding.^[8,9] The iron ore concentrate used in this study contained 1.4 pct coke breeze, which has been a standard

energy-saving practice at the majority of the pelletizing plants in Quebec.

B. Green Ball Formation and Induration

By using a disc pelletizer of 29-cm diameter at an inclination of 42 deg at 20 rpm, green balls were prepared. With these balling conditions, approximately 90 pct of the pellets produced falls in the size range of 10 to 15 mm in diameter. The green balls were dried in an oven at 383 K. The pellets were fired in a Lindberg furnace which was programmed to reach the firing temperature of 1573 K. Figure 1 shows the pattern of thermal treatment and relationship between time and temperature. In all the figures, the temperature is expressed in degrees Celsius. This can be converted to Kelvin by using the conversion equation $K = ^\circ\text{C} + 273.15$. For the raw materials used in this study, the weight loss as a function of time and temperature is shown in Figure 2.

For pellets produced with only limestone and bentonite addition at basicities of 1.3 and 1.6, the firing temperature was reduced from 1573 to 1548 K to avoid sticking due to partial melting of the pellets.

C. Testing of Pellets

Due to the limited quantity of pellets produced in each category, only some of the essential pellet properties were determined. These included compression strength,

Table II. Pellet Designation and Weight Percent of Binders and Fluxes in Green Pellet Mix (Dry Basis)

Basicity CaO + MgO SiO ₂ + Al ₂ O ₃	Pellet Type	Binder/Flux (Wt Pct)			
		Bentonite	Peat Moss (55 Pct H ₂ O)	Dolomite	Limestone
0.2	DB	1.0	—	1.8	—
	DP	—	3.0	1.8	—
0.8	DB	1.0	—	9.0	0.1
	DP	—	3.0	9.0	—
	LB	1.0	—	—	8.9
	LP	—	3.0	—	7.4
1.3	DB	1.0	—	9.0	6.4
	DP	—	3.0	9.0	3.7
	LB	1.0	—	—	14.9
	LP	—	3.0	—	12.8
1.6	DB	1.0	—	9.0	10.5
	DP	—	3.0	9.0	6.8
	LB	1.0	—	—	18.7
	LP	—	3.0	—	16.1

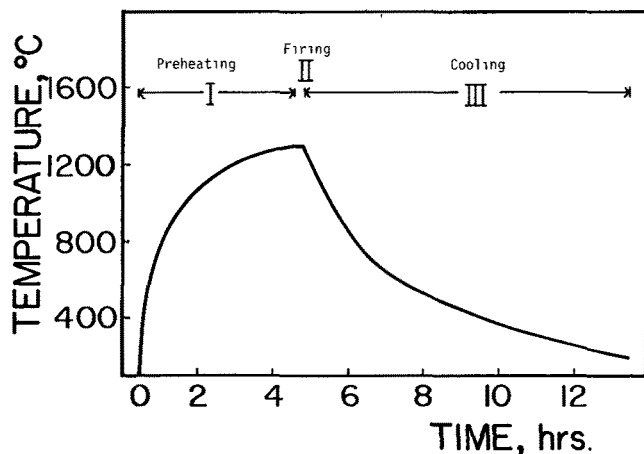


Fig. 1—Pattern of thermal treatment and relationship between time and temperature.

isothermal reduction behavior at 1223 K,^[11] swelling characteristics at 1223 K,^[12] and porosity.^[13]

D. Mineralogical Observation and Microanalysis

For examination of the microstructure of fired pellets, polished sections were prepared for observation under a reflected light metallurgical microscope. The proportion

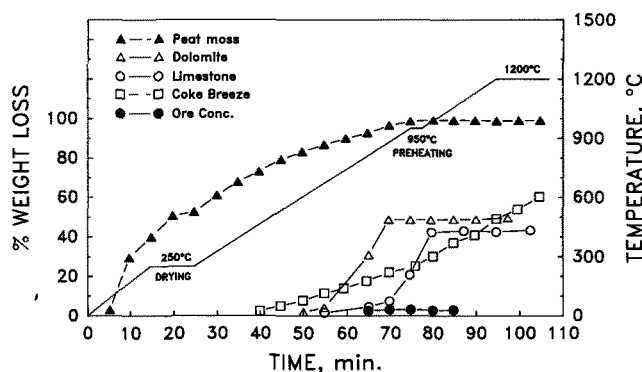


Fig. 2—Weight loss as a function of time and temperature of the raw materials used.

of various mineralogical phases was determined semi-quantitatively using an IBAS interactive image analysis system. The distribution of major metallic elements, namely, Fe, Ca, Si, Al, and Mg, in the crystalline and the bonding phases was determined semiquantitatively using a JEOL JSM 820 scanning electron microscope with energy dispersive spectrometer.

III. RESULTS AND DISCUSSION

The chemical compositions of fired pellets are given in Table III. It is generally noted that pellets produced with only limestone and bentonite tend to have a comparatively high FeO content as compared to other types of pellets. It is believed that in these pellets, because of comparatively low porosity and intergranular slag enveloping the magnetite phase, the magnetite phase does not get sufficiently reoxidized to hematite, thus resulting in a higher FeO content. It is also believed that as the slag-forming conditions are better with limestone and bentonite, a certain part of the FeO may have been retained in the slag phase.

It is noted from Table III that pellets produced with peat moss addition have slightly higher Fe content, since the chemical contamination resulting from peat moss is negligible.

A. Pellet Mineralogy and Bonding Mechanism

The major mineralogical phases observed in these pellets are hematite, magnetite, magnesioferrite, calcium ferrite, and glass. Hematite was the predominant phase; all other phases varied widely, depending on the basicity, type of flux, and binder.

The results of microprobe analysis are given in Tables IV through VII. The analyzed elements are presented in the respective oxide form in which they actually exist in the pellets. Since Fe exists in both ferric and ferrous states and the determination of their respective state is difficult, it is assumed that all Fe existed in ferric state unless otherwise specified. Average compositions of major crystalline phases present in all types of pellets are given in Table IV.

Table III. Chemical Composition of Fired Pellets

Basicity	Pellet Designation	Fe Total	FeO	SiO ₂	Al ₂ O ₃	CaO	MgO	Na ₂ O + K ₂ O	TiO ₂
0.2	DB	64.50	0.13	5.75	0.35	1.55	0.49	0.08	0.10
	DP	64.81	0.30	4.95	0.42	1.25	0.47	0.11	0.10
0.8	DB	63.00	<0.05	5.30	0.32	2.05	2.10	0.09	0.08
	DP	62.58	0.05	4.95	0.40	2.40	2.05	0.10	0.09
	LB	62.17	2.89	5.70	0.45	5.15	0.13	0.06	0.09
	LP	62.50	1.92	5.45	0.45	4.55	0.37	0.09	0.19
1.3	DB	59.09	<0.05	6.05	0.50	6.30	2.48	0.06	0.13
	DP	61.29	0.27	4.92	0.40	4.65	2.03	0.08	0.09
	LB	59.88	4.84	5.95	0.65	7.85	0.14	0.04	0.09
	LP	60.80	0.13	4.95	0.35	7.00	0.12	0.15	0.08
1.6	DB	58.16	0.13	5.55	0.45	8.25	1.86	0.05	0.17
	DP	59.36	0.13	4.72	0.33	6.10	2.11	0.06	0.09
	LB	59.41	0.20	5.05	0.40	9.05	0.18	0.06	0.06
	LP	60.87	<0.05	4.50	0.25	7.65	0.13	0.08	0.09

Table IV. Average Composition of Major Crystalline Phases Other than Magnesioferrite (SEM-EDS)

Mineralogical Phase	Fe ₂ O ₃	SiO ₂	CaO	MgO	Al ₂ O ₃	Remarks
Hematite (H)	99.50	0.39	0.10	—	—	all types of pellets
Hematite (H) (crystallized in slag)	95.73	1.70	2.45	0.03	0.09	all types of pellets
Magnetite (M)	97.07	0.52	1.52	0.70	0.20	only limestone-fluxed pellets
Calcium ferrites (CF)	80.18	5.92	12.73	0.14	1.03	observed only at <i>B</i> = 1.3 and 1.6
Calcium ferrites (CF) (crystallized in slag)	71.85	10.42	16.69	0.45	0.59	observed in pellets <i>B</i> ≥ 0.8

Table V. Average Composition of Glass Phase in Limestone-Fluxed Pellets (SEM-EDS)

Basicity	Pellet Designation	Fe ₂ O ₃	SiO ₂	CaO	MgO	Al ₂ O ₃
0.8	LB	11.64	41.33	46.71	—	0.62
		27.61	34.69	36.61	0.12	0.97
	LP	17.66	36.94	45.40	—	—
		39.04	33.39	24.48	1.70	1.38
1.3	LB	13.44	32.54	53.72	—	—
		26.21	26.20	44.09	0.61	1.99
	LP	9.46	33.49	56.98	0.02	0.03
		36.00	27.35	36.09	0.18	0.20
1.6	LB	10.12	28.00	61.34	—	0.85
		29.90	23.35	46.69	—	0.31
	LP	13.64	29.75	56.27	0.18	0.11
		33.01	22.77	43.78	—	0.20

Table VI. Average Composition of Glass Phase in Dolomite-Fluxed Pellets (SEM-EDS)

Basicity	Pellet Designation	Glass Phase (Zoned/Single*)	Fe ₂ O ₃	SiO ₂	CaO	MgO	Al ₂ O ₃	Relative Proportion in Glass Phase
0.2	DB	zoned pale gray	34.05	46.14	15.11	3.33	1.37	80 pct
		zoned dark	28.45	57.39	11.66	1.35	1.13	20 pct
0.8	DP	zoned pale gray	42.19	33.78	20.67	2.73	0.63	70 pct
		zoned dark	27.84	46.68	24.80	—	0.68	30 pct
1.3	DB	zoned pale gray	40.30	25.13	32.17	1.63	0.77	50 pct
		zoned dark	17.60	38.60	43.80	—	—	20 pct
		single	15.30	29.74	53.27	0.99	0.70	30 pct
1.6	DB	zoned pale gray	33.63	26.41	38.11	1.05	0.81	25 pct
		zoned dark	21.47	32.05	45.45	0.36	0.68	15 pct
		single	10.18	29.81	57.96	1.51	0.54	60 pct

*Glass phase in which no zoning is observed.

Table VII. Average Composition of Magnesioferrite in Dolomite-Fluxed Pellets (SEM-EDS)

Basicity	Pellet Designation	Fe ₂ O ₃	SiO ₂	CaO	MgO	Al ₂ O ₃	Occurrence* (Pct Pellet Matrix Exclusive of Pores)
0.2	DB	96.11	—	0.17	3.65	0.08	very little
	DP	—	—	—	—	—	not observed
0.8	DB	89.92	1.32	0.04	8.33	0.03	8 pct
	DP	91.29	0.81	0.43	7.36	0.12	9 pct
1.3	DB	90.96	0.94	1.62	6.30	0.18	11 pct
	DP	91.89	0.33	1.28	6.36	0.14	10 pct
1.6	DB	91.74	0.39	1.61	5.86	0.40	15 pct
	DP	93.72	0.12	1.30	4.76	0.10	17 pct

*Surface area measurement by IBAS interactive image analysis system (numbers are area percentages).

Two different types of glass phase were noticed in these pellets; (1) a zoned glass phase consisting of pale gray and dark and (2) a single dark phase as seen under reflected light. They were found to differ in composition, especially in the content of Mg and Fe. In the zoned glass phase, the pale gray phase was rich in Fe and Mg. However, with increased basicity from 0.8 to 1.6, the Fe and Mg content decreased, as did the proportion of zoned to the single silicate phase. Since the pale gray phase contained more Mg, this phase was predominant in dolomite-added pellets. Table V shows the most characteristic composition of the two types of glass phases in the order of their importance in limestone-fluxed pellets. Table VI shows the average composition of the zoned and single silicate phases in dolomite-fluxed pellets. Since the composition did not vary much with the type of binder, the composition for either bentonite- or peat moss-added pellet is given at any given basicity. It is evident that the zoned glass phases have a relatively high iron content, more iron being present in the pale gray than in the dark phase. Similar observations were made by Nekrasov *et al.*,^[1] and they described the phase as an association of wollastonite with hematite.

It is quite apparent that due to the presence of magnesia, there is an unusual zoning in the distribution of the type of silicate bond and magnesium over the pellet cross section.

In the pellets with dolomite addition, some magnesioferrites were formed which do not conform to the stoichiometric composition ($\text{MgO}\cdot\text{Fe}_2\text{O}_3$), being a phase which is highly deficient in MgO. Paladino^[14] has shown the existence of spinel (magnesioferrite) compositions which lie between $\text{MgO}\cdot\text{Fe}_2\text{O}_3$ and Fe_2O_3 , *i.e.*, in the high-iron portion of the spinel field where excess spinels exist. It is expected that vacancies would occur in the iron lattice as in magnetite. The work of Koizumi and Roy^[15] also had shown that solid solubility of Fe_2O_3 in $\text{MgO}\cdot\text{Fe}_2\text{O}_3$ is temperature-dependent, being essentially zero at near 1073 K and 90 mole pct at about 1648 K. These investigations clearly indicate the existence of magnesioferrite compositions which are highly deficient in MgO. From our investigation, it is believed that under localized reducing conditions, primarily due to incorporation of coke breeze in the mix, initially the complex spinel of the type $((1-x)\text{Mg}\cdot x\text{Fe})\text{O}\cdot\text{Fe}_2\text{O}_3$ was formed. During cooling under oxidizing conditions, these spinels dissociated into magnesioferrite, which is deficient in MgO, and the ferrous iron changed into ferric state to form Fe_2O_3 . However, elucidation of the exact mechanism of formation of magnesioferrite in these types of pellets requires further investigation.

Microanalysis of the magnesioferrite showed the presence of varied amounts of SiO_2 and CaO, depending on the local chemistry, and certain amounts of diluted MgO with increased basicity (Table VII).

1. Basicity 0.2

Typical photomicrographs of pellets at the basicity of 0.2 with bentonite and peat moss addition are shown in Figure 3. On account of very low flux addition at this basicity (*i.e.*, acid pellets), the bonding is provided by a consolidation of crystal bridges formed by small and ultrafine particles and bridging of relatively large he-

matite crystals by a thin film of slag. The slag formation took place due to incipient agglomeration of ultrafine concentrates, gangue, and flux during pellet induration. A part of the ultrafine hematite recrystallized from the melt. The pellet structure was dominated by pores. With peat moss addition, more pores were formed, and the structure appeared more open-textured. The presence of free silica was often observed in the pellets (Figure 3(a)), showing its inertness at this basicity. Microprobe analysis showed that the composition of slag did not differ very much with the type of binder but varied depending on the type of silicate phase.

2. Basicity 0.8

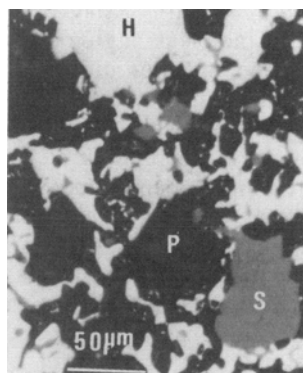
Typical photomicrographs of pellets with bentonite and peat moss additions are shown in Figures 4 and 5. At this basicity, due to increased flux addition, the bonding by slag becomes imminent. The formation of slag in the porous structures and consolidation of pellets are due to surface tension forces operating through the increasingly fluid medium bringing the ore particles closer. However, it was observed that the decrease in porosity is still only marginal. It is presumed that following calcination of flux and their subsequent assimilation into the slag phase, a large number of pores are left behind in the pellet structure, since only partial and localized melting takes place in the pellet mass during the process of induration.

The bond phase in the limestone-fluxed pellets with bentonite, as well as peat moss addition, consisted mainly of silicates formed from the melt, which were somewhat evenly distributed between the hematite crystals. The silicate bond was found to be highly heterogeneous in its mineral composition and structure. A small percentage of bonding phase was found to be calcium ferrites approaching the range of compositions of silicoferrites of calcium and aluminum (SFCA). The main difference between bentonite- and peat moss-added pellets was in the degree of porosity, which is much higher in the peat moss-added pellets.

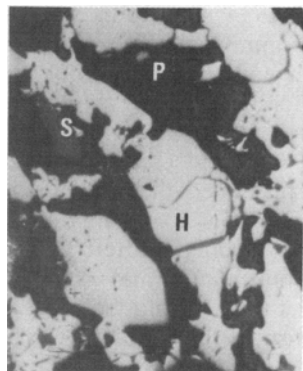
In pellets produced with dolomite addition, some magnesioferrite was formed, as described earlier. A typical SEM photomicrograph (secondary electron) of major mineralogical phases is shown in Figure 6. The microanalysis of these phases is given in Table VIII. The analysis shows that magnesioferrites contain between 7 and 9 pct MgO, with varied quantities of SiO_2 and CaO. As noted earlier, zoning of slag phase was quite evident: (1) the pale gray phase is high in Fe_2O_3 and MgO, and (2) the dark phase is high in SiO_2 and CaO but low in Fe_2O_3 , with virtually no MgO. Since MgO increases the liquidus temperature of the slag phase, relatively less slag was formed during induration. The distribution of Fe, Ca, Mg, Si, and Al in the bonding phase varied widely, indicating that only localized melting has taken place. With peat moss addition, even though more pores were distributed in the pellet matrix, the elemental distribution in the bonding phase did not show any significant change.

3. Basicity 1.3

In the pellets with limestone and bentonite addition, the formation of calcium ferrites, particularly around pores, was noted (Figure 7(a)). The predominant crystalline phase was hematite. Magnetite amounted to approximately 10 pct, correlating well with the relatively



(a) DB



(b) DP

Fig. 3—Photomicrographs of pellets fluxed with dolomite: (a) DB and (b) DP ($B = 0.2$). Symbols used for identification of mineralogical phases are H—hematite, S—free silica, and P—pore.

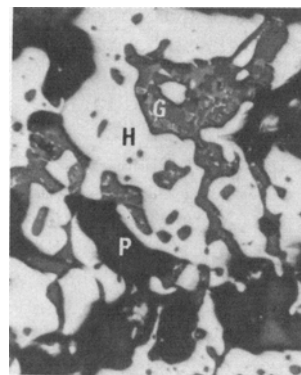
high FeO content noted for these pellets. The bonding phase consisted of (1) silicates with a varied distribution of Fe, Ca, Si, Mg, and Al and (2) a small amount of calcium ferrites with a varied distribution of Si and Al.

Pellets with dolomite addition exhibited very little formation of calcium ferrites; the phase which resembled magnetite was essentially magnesioferrites (Figure 8(a)) of the type described earlier. The bonding silicate phase displayed zoning. The pale gray phase contained a high percentage of Mg and Fe, and the dark phase was relatively low in both of these elements but high in Si and Ca. Peat moss-added pellets in both cases showed similar mineral assemblage but with a highly porous structure (Figures 7(b) and 8(b)).

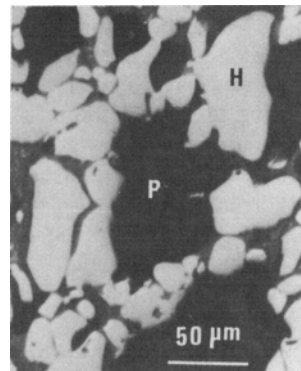
4. Basicity 1.6

At this basicity, pellets produced with limestone and bentonite exhibited appreciable calcium ferrite formation (Figure 9(a)). Hematite still dominated the pellet structure. Unlike the pellets at the basicities of 0.8 and 1.3, the magnetite formation was significantly reduced. The bonding phase primarily consisted of calcium ferrites and, to a lesser extent, of silicate glass phase.

Peat moss addition resulted in significant decrease in the calcium ferrite formation. The primary bonding was by silicate glass phase, with precipitation of small hematite crystals (Figure 9(b)). A significant amount of



(a) LB



(b) LP

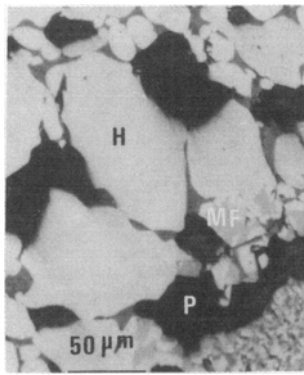
Fig. 4—Photomicrographs of pellets fluxed with limestone: (a) and (b) LP ($B = 0.8$). Symbols used for identification of mineralogical phases are H—hematite, G—glass (single), and P—pore.

hematite was retained in the glass phase. At this basicity the pellet structure appeared to be more consolidated compared to the peat moss-added pellets at other basicities.

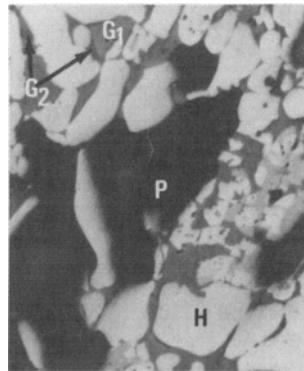
Pellets with dolomite and bentonite addition exhibited similar mineralogical assemblage, as in the case 1.3, but with much less zoning in the bonding phase. A typical pellet structure depicting the presence of magnesio-ferrite and the formation of lamellar hematite on magnesio-ferrites is shown in Figure 10(a). With peat moss addition, the mineralogical makeup was the same, but the pellet structure showed a high degree of pore formation (Figure 10(b)). At this basicity, free silica was absent, indicating that all the silica present in the concentrate was fully assimilated into the melt.

B. Pellet Physical and Reduction Properties

The results of the tests conducted on these pellets are given in Table IX. It should be noted that it is difficult to produce pellets of acceptable green strength characteristics in a laboratory disc, since the pellets are not compacted to a similar extent, as would be expected for a much larger disc in a pelletizing industry or pilot plant. Tests carried out on pilot scale on similar pellets made earlier¹⁶ have shown that both good green strength and



(a) DB



(b) DP

Fig. 5—Photomicrographs of pellets fluxed with dolomite: (a) DB and (b) DP ($B = 0.8$). Symbols used for identification of mineralogical phases are H—hematite, MF—magnesioferrite, G_1 —glass (pale gray), G_2 —glass (dark), and P—pore.

fired strength can be obtained. The results reported here indicate inferior compression strength and very high porosity, reflecting a low degree of compaction in most of these pellets. The pellet physical and reduction properties given here are, therefore, intended to show the trend.

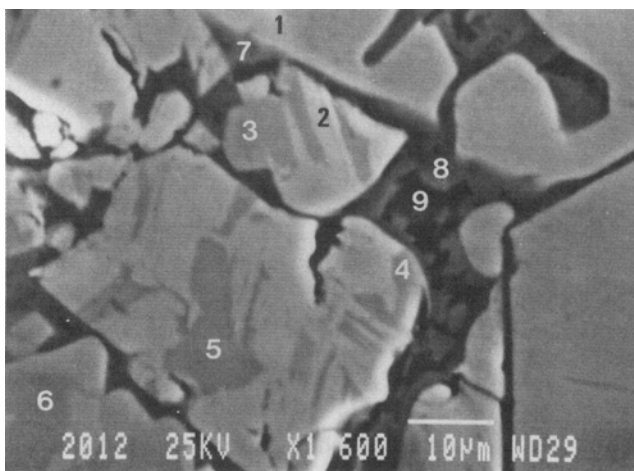
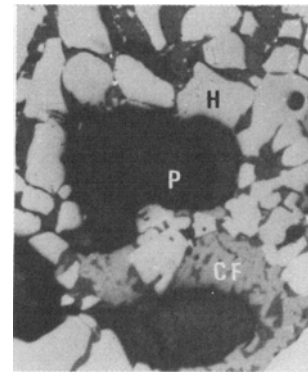
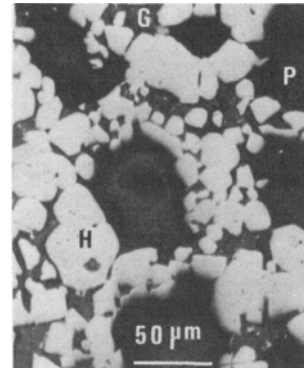


Fig. 6—Electron micrograph of pellets fluxed with dolomite ($B = 0.8$).



(a) LB



(b) LP

Fig. 7—Photomicrographs of pellets fluxed with limestone: (a) LB and (b) LP ($B = 1.3$). Symbols used for identification of mineralogical phases are H—hematite, CF—calcium ferrite, G—glass (single), and P—pore.

1. Porosity

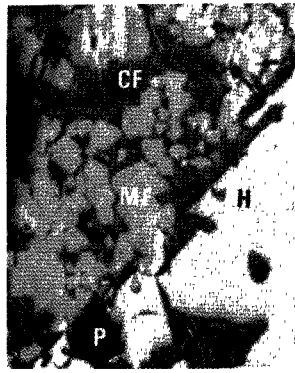
The variation of porosity as a function of basicity and pellet type is shown in Figure 11.

Pellets produced with peat moss, irrespective of flux type, tend to have high porosity, caused by burning of peat moss before any liquid-phase formation has taken place (Figure 2). During induration, insufficient liquid phase is formed to fill in the extra pores.

At high basicities, due to higher availability of CaO,

Table VIII. Microanalysis of Mineralogical Phases as shown in Figure 6 (Dolomite/Bentonite Pellet at $B = 0.8$)

No.	Mineralogical Phase	Fe ₂ O ₃	SiO ₂	CaO	MgO	Al ₂ O ₃
1	H	99.12	0.81	0.07	—	—
2	H (reoxidized)	98.52	1.02	0.47	—	—
3	MF	90.98	0.90	0.02	8.80	—
4	MF	91.17	1.07	0.10	7.76	—
5	MF	86.97	2.98	1.05	9.01	—
6	MF	90.52	1.10	0.29	8.08	0.01
7	G_1 (pale gray)	39.24	35.26	21.42	3.88	0.20
8	G_1 (pale gray)	33.30	37.99	21.84	4.63	2.24
9	G_2 (dark)	16.24	48.53	34.35	—	0.88

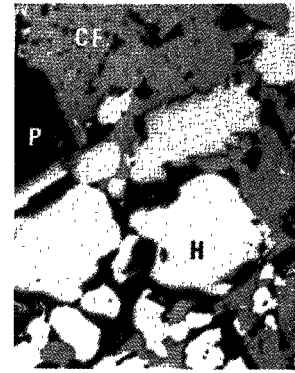


(a) DB

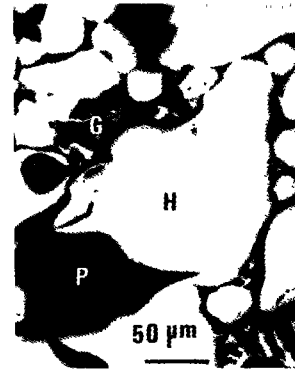


(b) DP

Fig. 8—Photomicrographs of pellets fluxed with dolomite: (a) DB and (b) DP ($B = 1.3$). Symbols used for identification of mineralogical phases are H—hematite, MF—magnesioferrite, CF—calcium ferrite, and P—pore.



(a) LB



(b) LP

Fig. 9—Photomicrographs of pellets fluxed with limestone: (a) and (b) LP ($B = 1.6$). Symbols used for identification of mineralogical phases are H—hematite, CF—calcium ferrite, G—glass (gle), and P—pore.

more liquid phase is formed during induration, thus filling in some of the pores created by the burning of peat moss. The results obtained also reflect this trend.

It is also seen from Table IX that dolomite addition results in higher porosity in comparison to limestone addition. MgO, being a major constituent of dolomite, raises the liquidus temperature of slag.^[17] Thus, there is less liquid formation at the induration temperature.

2. Compression Strength

Porosity appears to have a major influence on the compression strength of pellets (Figure 12). Pellets having high porosity generally have low strength, *viz.*, the pellets with dolomite and peat moss addition. The strength improves with increasing basicity, resulting from consolidation of the pellet bonds and decreased porosity. The variation of pellet compression strength with basicity for all the types of pellets is shown in Figure 13.

3. Reducibility

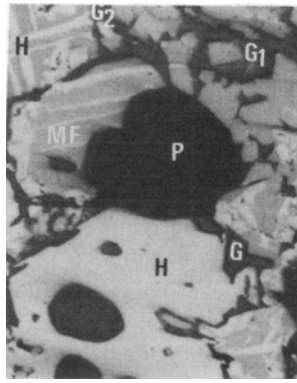
The variation of reducibility with basicity and pellet type is shown in Figure 14. It is noted that the reducibility reaches a maximum at basicity 1.3 and then decreases with increased basicity.

To understand this phenomenon, the pellets were re-

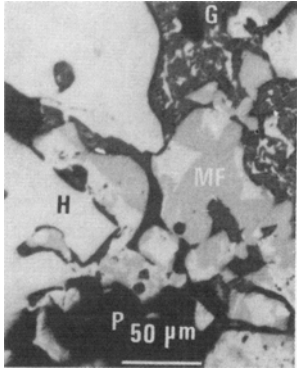
duced for 15, 30, 45, and 60 minutes, keeping the reduction conditions constant. A study of the microstructure of these reduced pellets revealed that in all the pellets, hematite-to-wustite transformation was complete during the initial 15 minutes. As the reduction time was increased, the extent of reduction from wustite iron varied depending on the basicity and type of pellet. The observations made and reduction mechanisms at different basicities are given below:

(a) At basicities ≤ 0.8 , the primary hematite grains were present in the unreduced sample have broken down to smaller grains during the initial stages of reduction (Figure 15). This may be ascribed to the breakdown of large hematite grains during the transformation to magnetite and along the boundaries of impurities and/or imperfections. As the reduction proceeds, nucleation of metallic iron takes place along the peripheral region and proceeds inwardly. However, even after 60 minutes' reduction, a substantial amount of wustite is still unreduced. According to St. John *et al.*,^[18] with very low CaO in the solid solution with wustite, a dense interlayer is formed during the reduction of wustite to iron thus slowing down the reduction of wustite toward the interior.

(b) On the other hand, at the basicity 1.3, due to



(a) DB



(b) DP

Fig. 10—Photomicrographs of pellets fluxed with dolomite: (a) DB and (b) DP ($B = 1.6$). Symbols used for identification of mineralogical phases are H—hematite, MF—magnesioferrite, G—glass (single), G_1 —glass (pale gray), G_2 —glass (dark), and P—pore.

attack of basic fluxes, in particular CaO, the grain size of hematite is relatively small in the unreduced pellet. This provides a much larger surface from an initial reduction point of view. It was also noted that fine intragranular pores existed in the wustite phase following the

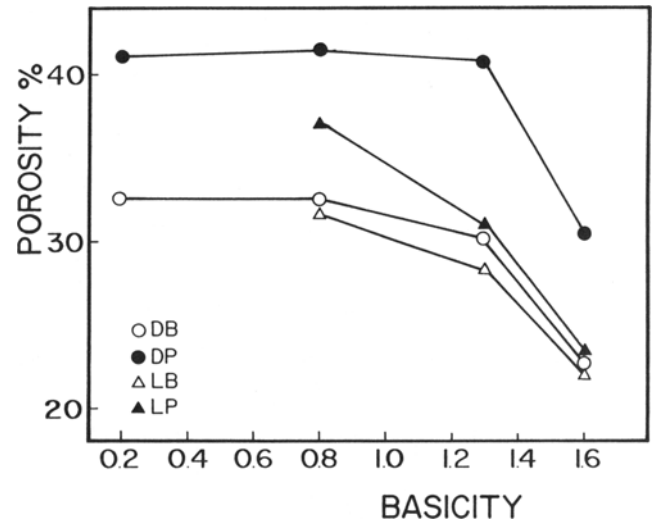


Fig. 11—Variation of porosity as a function of basicity and pellet type.

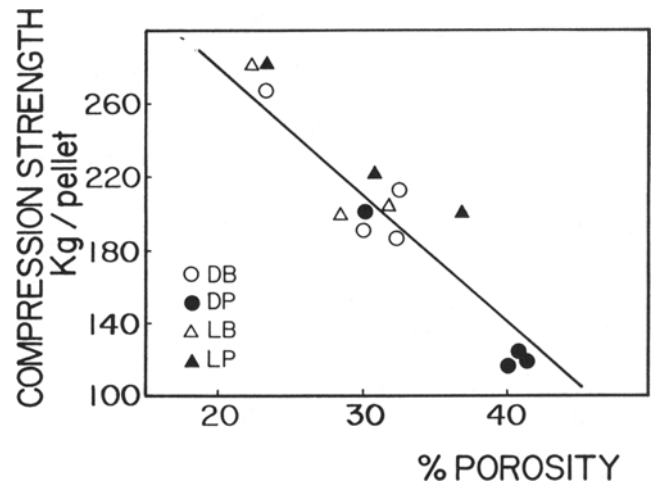


Fig. 12—Relationship between compression strength and porosity.

Table IX. Physical and Reduction Properties of the Pellets Produced

Basicity	Pellet Designation	Porosity (Pct)	Compression Strength (kg/Pellet)	Reducibility (dR/dt) ₄₀ (Pct Reduction/min)	Maximum Swelling (Pct)
0.2	DB	32.50	186.4	0.49	25.40
	DP	40.09	115.9	0.60	23.35
0.8	DB	32.72	195.6	0.62	28.46
	DP	41.14	120.4	0.82	24.35
	LB	31.71	204.5	0.64	31.23
	LP	37.04	210.6	0.76	24.79
1.3	DB	30.25	190.9	1.34	11.47
	DP	40.91	127.2	1.75	21.99
	LB	28.44	200.0	1.24	26.64
	LP	30.92	222.7	1.27	16.34
1.6	DB	23.55	268.7	0.83	12.66
	DP	30.34	200.0	1.40	10.52
	LB	22.65	279.5	0.73	12.33
	LP	23.65	281.8	0.75	12.66

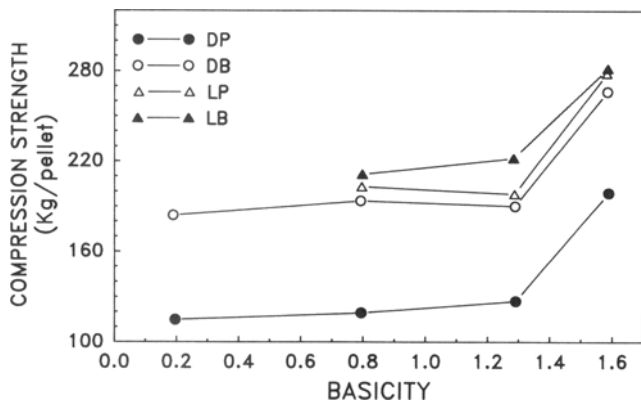


Fig. 13—Variation of compression strength as a function of basicity and pellet type.

initial reduction stage (Figure 16). Metallic iron nucleated along the fine pores, and after 45 minutes' reduction time, most of the wustite has been reduced to metallic iron. Another mechanism, as proposed by Nakiboglu *et al.*^[19] during the reduction of wustite to iron, may also prevail. It has been suggested that due to the presence of CaO in solid solution in wustite, porous iron morphologies are obtained as the final reduction product as compared to purer wustite (*e.g.*, occurring at low basicity), on which a dense iron layer is formed.

(c) At the basicity 1.6, it is noted that in unreduced pellets, a predominantly secondary hematite phase exists. These secondary hematite crystals are often found to be large due to the coalescence of smaller hematite grains in a larger fluid medium during the induration process. In this case, therefore, the reduction mechanism in the initial stages is somewhat similar to that at low basicities. However, following 15 minutes' reduction time, the formation of the fine pores in the wustite was very predominant. Toward the later stage of reduction, *i.e.*, from wustite to iron, the mechanism of reduction as explained for basicity 1.3 prevailed.

The excellent reduction properties exhibited by pellets produced with dolomite and peat moss addition at the basicity 1.3 are mainly attributable to high porosity and

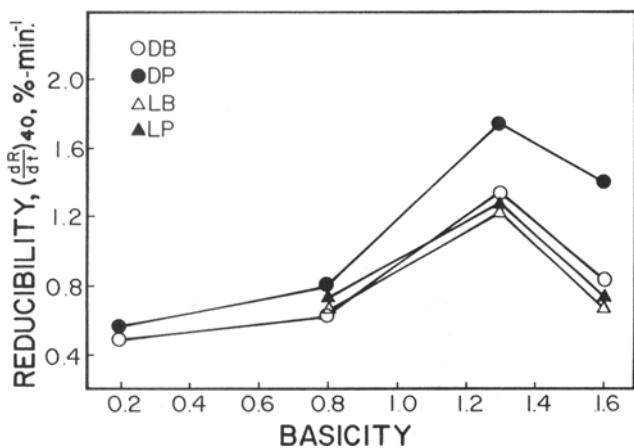
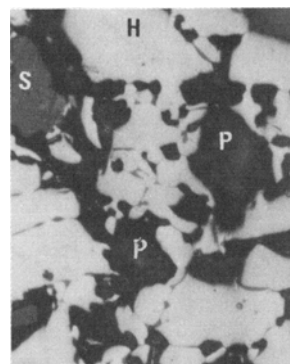
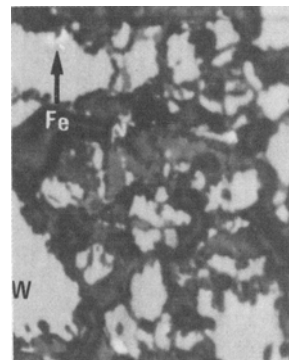


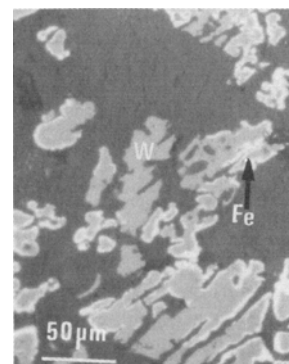
Fig. 14—Variation of reducibility as a function of basicity and pellet type.



(a) unreduced



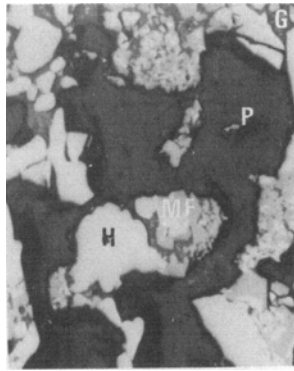
(b) 30 min. reduction



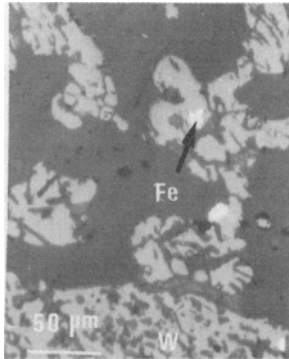
(c) 45 min. reduction

Fig. 15—Photomicrographs of partially reduced DP pellets at basicity 0.2. Symbols used for identification of mineralogical phases: H—hematite, W—wustite, Fe—metallic iron, S—free silica, P—pore.

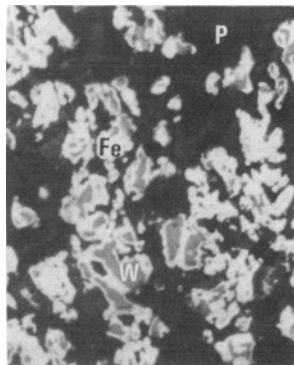
the phenomenon observed above. It is believed that combination of these two factors provides easy accessibility of the reducing gases to the iron oxide surface. Despite the fact that at lower basicities ($B \leq 0.8$) porosity of the pellets is quite high, low reducibility noted for these pellets. It is believed that in addition to the phenomenon explained above, the free silica and F react to form a fayalitic melt. The partial redistribution of this melt among iron oxide grains severely reduces gas permeability and consequently lowers the rate of further pellet reduction. In the presence of alkali



(a) un-reduced



(b) 15 min. reduction



(c) 45 min. reduction

Fig. 16—Photomicrographs of partially reduced DP pellets at basicity 1.3. Symbols used for identification of mineralogical phases are H—hematite, W—wustite, Fe—metallic iron, G—glass (single), and P—pore.

compounds, particularly of Na and K, melt formation is further promoted, and this severely restricts the reduction of iron oxides. On the other hand, at basicity 1.6, the significant decrease in the porosity in association with the fact that large coalesced hematite crystals result in a lower reducibility.

In general, the lower reducibility observed for limestone- and bentonite-added pellets may be ascribed to relatively lower porosity and increased FeO content in the pellet. Mineralogical study indicates that a relatively higher amount of magnetite is present in these pel-

lets, and a certain amount of slag envelops the iron oxide phase. This decreases the accessibility of the iron oxides to reducing gases. At the basicity 1.6, formation of calcium ferrites at the expense of highly reducible hematite may have contributed to relatively low reducibility of these pellets.

To further account for the difference in reduction behavior of pellets at different basicities, a more systematic study involving the effect of CaO and MgO on the reduction mechanism is required.

4. Swelling

The results indicate that maximum swelling occurred at the basicity of 0.8 and was greatly enhanced for pellets produced with limestone and bentonite addition (Table IX). In general, it is also noted that with peat moss addition, the swelling reduces considerably. High porosity in the peat moss-added pellets appears to have a favorable influence on the swelling characteristics.^[8]

Increased flux addition helps in bringing down the swelling to considerably lower levels. Earlier studies^[16,17] also confirm this trend. This is primarily attributed to a stronger bonding phase which is able to absorb the stress during the transformation of hematite to magnetite.

IV. CONCLUSIONS AND RECOMMENDATIONS FOR INDUSTRIAL PRACTICE

1. The bonding in fluxed pellets produced from specular hematite consists of two silicate phases: (1) a zoned glass phase consisting of magnesian-ferruginous and the other with very little or no magnesium and low iron, and (2) a single glass phase containing high quantities of silicon, calcium, and aluminum.
2. With increasing basicity, the solubility of iron oxides in the melt and the quantity of the magnesian-ferruginous phase decrease.
3. Although the presence of calcium ferrites is noticed at the basicity of 0.8, no appreciable formation takes place until a basicity of 1.6. Appreciable amounts of calcium ferrites are formed only in pellets produced with limestone and bentonite addition. The bonding of pellets at the basicity 1.6 takes place by (1) glass and, to a lesser extent, by magnesian-ferruginous silicates, and (2) calcium ferrites.
4. Melt formation during pellet induration through the additions of fluxes has a great influence on the metallurgical properties of pellets. With the increased basicity, while there is an improvement in terms of pellet strength and swelling characteristics, well-balanced metallurgical properties are obtained at the basicity 1.3.
5. Dolomite addition is necessary to maintain a balance between various pellet properties.
6. Pellet reduction properties can be enhanced by incorporating peat moss as a binder, although such additions result in weakening of the pellets.
7. High limestone addition can be tolerated if peat moss is used as a binder and the problem of pellet sticking can be minimized.

ACKNOWLEDGMENTS

The authors wish to extend their sincere appreciation to the Quebec Ministry of Energy Resources, Centre for Mineral Research, Ste. Foy, PQ, Canada for financial support. A part of this work was presented at the W.O. Philbrook Memorial Symposium (AIME-ISS) held in Toronto during April 1988.

REFERENCES

1. Z.I. Nekrasov, G.M. Drozdov, Y.S. Shmelev, M.G. Boldenko, and Y.G. Danko: *Steel USSR*, 1978, vol. 8 (8), pp. 429-35.
2. K. Meyer: *Pelletization of Iron Ores*, Springer-Verlag, Berlin, 1980, pp. 41-46, 121-26, and 151-53.
3. J.D.G. Hamilton: *Trans. Inst. Min. Metall., Sect. C*, 1976, vol. 85 (3), pp. C30-39.
4. M.C. Chang and D.B. Malcom: Proc. ISCTIC, *Trans. Iron Steel Inst. Jpn., Suppl.*, 1971, vol. 11, pp. 66-70.
5. C.G. Thomas, J.D.G. Hamilton, and K.McG. Bowling: *The Aus. I.M.M., Newcastle and District Branch, Pellets and Granules Symp.*, Australas. IMM, Melbourne, Australia, Oct. 1974, pp. 93-106.
6. M. Sasaki, T. Nakazawa, and S.I. Kondo: *Trans. Iron Steel Inst. Jpn.*, 1968, vol. 8, pp. 146-55.
7. D.M. Urich and T.-M. Han: *Agglomeration*, W.A. Knepper, ed., Interscience Publisher, New York, NY, 1962, pp. 669-719.
8. S.C. Panigrahy, M. Rigaud, I. Malinsky, and R. Tremblay: *4th Int. Symp. on Agglomeration*, Toronto, ON, Canada, I. AIME, Warrendale, PA, 1985, pp. 75-82.
9. R. Tremblay: *Annual CIM Conf. of Metallurgists*, Quebec, I. Canada, CIM, Montreal, PQ, Canada, Aug. 1984.
10. *Iron Ore Pellets—Determination of Crushing Strength*, ISO/47 International Organization for Standardization, Geneva, Switzerland, 1983.
11. *Iron Ore Determination of Reducibility*, ISO/4695, International Organization for Standardization, Geneva, Switzerland, 1984.
12. M. Jallouli, M. Rigaud, and F. Ajersch: *3rd Int. Symp. Agglomeration*, NMA Nürnberger Messe-Und Ausstellgesellschaft Messezentrum, Nuremberg, Federal Republic Germany, 1981, pp. B81-103.
13. S.C. Panigrahy, M. Jallouli, and M. Rigaud: *Ironmaking Proc* 1984, vol. 43, pp. 233-40.
14. A.E. Paladino: *J. Am. Ceram. Soc.*, 1960, vol. 43 (pp. 183-91.
15. M. Koizumi and Rustum Roy: *60th Annual Meeting*, The American Ceramic Society, Pittsburgh, PA, Basic Science Div. 1 34-B-58, Apr. 1958.
16. M. Rigaud, B.C. Jena, S.C. Panigrahy, and G. Paquet: *Iron S. Soc. Trans.*, 1988, vol. 9, pp. 131-38.
17. K. Lingtan, Lu Yang, and W.-K. Lu: *Scand. J. Metall.*, 19 vol. 12, pp. 166-76.
18. D.H. St. John, S.P. Matthew, and P.C. Hayes: *Met. Trans. B*, 1984, vol. 15B, pp. 709-17.
19. F. Nakiboglu, D.H. St. John, and P.C. Hayes: *Met. Trans. B*, 1986, vol. 17B, pp. 375-81.